

# Uncertainty Modeling for Hard Disk Drives

Masanori Honda and Peter Seiler

**Abstract**—A modern hard disk drive uses a dual-stage actuator to read/write data on a track with width less than 100nm. The dual-stage actuator requires an advanced controller to achieve high performance on millions of hard disk drives. This paper presents a numerical algorithm utilizing convex optimization to create an uncertainty model, for the purpose of synthesizing a robust controller, from a set of experimental frequency response data. Furthermore several practical issues of constructing an uncertainty model for the dual-stage actuator are described. The proposed method is applied to a set of frequency response data of dual-stage actuators from numerous hard disk drives to create an uncertainty model of the actuator. Then the uncertainty model is used to synthesize a robust control law, which is implemented and experimentally tested on a hard drive.

## I. INTRODUCTION

A typical hard disk drive (HDD) works by spinning a magnetic disk while a magnetic head reads/writes data from/to circular tracks on the disk. Modern HDD have achieved significant improvements in data track density and historically the data density of disk drives has historically doubled almost every 2 years [1]. For example, one drive currently manufactured by Seagate has a track density of 340,000 tracks per inch, which translates to about 75nm per track [2]. Many modern HDDs utilizes a dual-stage actuator composed of a voice coil motor (VCM) and a micro actuator (MA) in order to improve tracking to keep up with the reduction in track width. The internal structure of a typical HDD, shown in Fig. 1, has the VCM located at the base of the actuator arm while the MA is located nearer to the magnetic head. The VCM is the primary actuator that provides a full range of motion for the magnetic head to cover all disk tracks. The MA provides greater tracking accuracy than the VCM but with a smaller range of motion.

Advanced controller for the dual-stage actuator is also required to achieve high performance across millions of HDDs, each of which has similar and yet unique dynamics.  $\mu$ -synthesis [3] is one technique that can be utilized to synthesize a robust controller. This method requires a model for the nominal actuator dynamics as well as the uncertainty associated with this nominal model. It is often difficult to analytically create an uncertainty model for a complex system such as a dual-stage actuator on a HDD. This paper describes an efficient algorithm to automatically construct an uncertainty set from an empirical frequency response data. The work in this paper builds upon several results in the existing literature. The most closely related results

are contained in [4] and [5]. Semidefinite programming (SDP) was used in [4] to construct an optimal uncertainty model from frequency response data accounting for both noise and fitting errors. A similar approach, presented in [5], forms the basis of the Matlab command `ucover`. The `ucover` function computes a minimal uncertainty bound from a given set of frequency response data and a known nominal model. The nominal model is typically computed by simply averaging the frequency response data. Approaches to construct uncertainty models from time domain data have also been presented in [6]–[9].

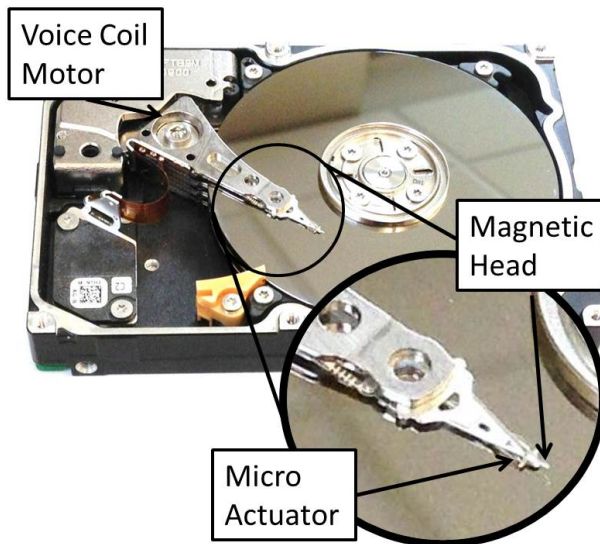


Fig. 1. Typical Internal structure of a HDD with a dual stage actuator.

This paper uses convex optimization to construct uncertainty sets from experimental frequency response data. The proposed algorithm generates both the nominal model and the uncertainty bounds from empirical frequency response data. It is shown via a simple example that optimizing the nominal model (rather than simply averaging the data) leads to a reduction in the uncertainty bounds. This ultimately reduces the conservatism in the control design. Several practical issues that arise in the construction of uncertainty sets for the dual-stage actuator application are also described. Finally, the proposed method is applied using data from many HDDs. The resulting uncertainty set is used to synthesize, implement, and experimentally test a robust control law.

## II. NOTATION

$\mathbb{R}$  and  $\mathbb{C}$  denote the sets of real and complex numbers, respectively.  $\mathbb{R}L_{\infty}$  denotes the set of rational functions with

real coefficients that are proper and have no poles on the imaginary axis.  $\mathbb{RH}_\infty$  is the subset of functions in  $\mathbb{RL}_\infty$  that are analytic in the closed right half of the complex plane.  $\mathbb{R}^{n \times m}$ ,  $\mathbb{C}^{n \times m}$ ,  $\mathbb{RL}_\infty^{n \times m}$  and  $\mathbb{RH}_\infty^{n \times m}$  denote the sets of  $n \times m$  matrices whose elements are in  $\mathbb{R}$ ,  $\mathbb{C}$ ,  $\mathbb{RL}_\infty$ ,  $\mathbb{RH}_\infty$ , respectively. A single superscript index is used for vectors, e.g.  $\mathbb{R}^n$  denotes the set of  $n \times 1$  vectors whose elements are in  $\mathbb{R}$ . For a matrix  $M \in \mathbb{C}^{n \times m}$ ,  $M^T$  denotes the transpose and  $M^*$  denotes the complex conjugate transpose. For a square matrix  $M \in \mathbb{C}^{n \times n}$ ,  $\text{Tr}[M]$  denotes the trace of the matrix  $M$ . For an LTI system  $G$ , the  $H_\infty$  norm is defined as  $\|G\| := \sup_\omega \bar{\sigma}(G(j\omega))$ .

### III. UNCERTAINTY MODELING

#### A. Problem Statement

The problem formulation assumes that a collection of  $n \times m$  frequency responses are obtained from input/output experiments. The  $k^{\text{th}}$  experimental dataset ( $k = 1, \dots, K$ ) consists of the complex frequency response data  $G_k := \{G_k(j\omega_1), \dots, G_k(j\omega_F)\} \subset \mathbb{C}^{n \times m}$  defined on a common grid of frequencies  $\{\omega_f\}_{f=1,2,\dots,F} \subset \mathbb{R}$ . This data can be easily and efficiently computed for many drives in the HDD application using a basic sinusoidal frequency sweep. For robust control design it is useful to construct an uncertainty set of linear, time-invariant models  $\mathcal{S} \subset \mathbb{RL}_\infty^{n \times m}$  that contains all the frequency response data. Specifically, the uncertainty set  $\mathcal{S}$  is said to cover the collection of experimental data if for each frequency response  $G_k$  there exists a model  $\tilde{G} \in \mathcal{S}$  such that  $\tilde{G}(j\omega_f) = G_k(j\omega_f)$  for all frequencies  $f = 1, \dots, F$ .

This paper focuses on two types of non-parametric uncertainty sets: additive and input multiplicative uncertainty. These uncertainty sets are both described by a nominal model  $G_0 \in \mathbb{RL}_\infty^{n \times m}$  and stable uncertainty weights  $W_L \in \mathbb{RH}_\infty^{n \times n}$ ,  $W_R \in \mathbb{RH}_\infty^{m \times m}$  where the dimensions of  $W_L$  depend on the uncertainty set type. The additive ( $\mathcal{S}_A$ ) and input multiplicative ( $\mathcal{S}_M$ ) uncertainty sets are defined as:

$$\mathcal{S}_A := \{G_0 + W_L \Delta W_R : \Delta \in \mathbb{RL}_\infty^{n \times m}, \|\Delta\| \leq 1\} \quad (1)$$

$$\mathcal{S}_M := \{G_0(I_m + W_L \Delta W_R) : \Delta \in \mathbb{RL}_\infty^{m \times m}, \|\Delta\| \leq 1\} \quad (2)$$

The dimensions of  $W_L$  are  $n \times n$  and  $m \times m$  for the additive and multiplicative uncertainty sets, respectively. The explicit dependence of the uncertainty set on the nominal model and weights will occasionally be denoted, e.g.  $\mathcal{S}_A(G_0, W_L, W_R)$ .

For a given type of uncertainty set (additive or input multiplicative), the objective is to construct the nominal model  $G_0$  and uncertainty weights  $W_L$  and  $W_R$  such that the resulting uncertainty set covers the collection of experimental data. In addition, the “smallest” possible uncertainty set that covers the data should be constructed since this will reduce the conservatism in the robust control design. The following function will be used as a measure for the size of the uncertainty set at the frequency  $\omega$ :

$$h(W_L, W_R, \omega) := \text{Tr}[W_L(j\omega)^* \Gamma_L W_L(j\omega)] + \text{Tr}[W_R(j\omega) \Gamma_R W_R(j\omega)^*] \quad (3)$$

where  $\Gamma_L$  and  $\Gamma_R$  are positive definite matrices of appropriate dimensions. These matrices are chosen to emphasize specific directions in the input/output space. They can also be chosen as functions of  $\omega$  to emphasize specific frequency bands. In most cases the simple choices  $\Gamma_L = I$  and  $\Gamma_R = I$  provide reasonable results. The following optimization is a formal statement for the uncertainty set construction problem:

$$\begin{aligned} \min_{G_0, W_L, W_R} \int_0^\infty h(W_L, W_R, \omega) d\omega \\ \text{subject to: } \mathcal{S}_A(G_0, W_L, W_R) \text{ covers } \{G_k\}_{k=1,\dots,K} \end{aligned} \quad (4)$$

The optimization is stated for additive uncertainty sets but a similar optimization can be formulated using an input multiplicative uncertainty set. The following section will describe a numerical algorithm to approximately solve the optimizations for both uncertainty set types using semidefinite programming (SDP) [10]. The use on non-parametric uncertainty sets leads to a computationally tractable algorithm for covering the frequency response data. The approach described in this paper can be extended to other frequency domain uncertainty sets including output multiplicative, inverse additive, and inverse (input or output) multiplicative models [3], [11].

It is worth noting that if the nominal function  $G_0$  is specified and held fixed in the optimization then the results in [4], [5] can be used to construct  $W_L$  and  $W_R$ . In particular, the algorithm described in [5] forms the basis for the Matlab function `ucover` which constructs uncertainty set weights if the nominal model and frequency response data is given. A contribution of this paper is to develop an algorithm that addresses the practical issues that arise in creating uncertainty models from frequency response data of dual-stage actuators from HDDs.

#### B. Numerical Algorithm

The constraint in Equation 4 can be reformulated in terms of a frequency-dependent matrix inequality via the following lemma.

*Lemma 1 ([5]):* Let  $\mathcal{S}_A(G_0, W_L, W_R)$  be an additive uncertainty set (Equation 1) defined by a nominal model  $G_0 \in \mathbb{RL}_\infty^{n \times m}$  and stable uncertainty weights  $W_L \in \mathbb{RH}_\infty^{n \times n}$ ,  $W_R \in \mathbb{RH}_\infty^{m \times m}$ . In addition, assume  $W_L$  and  $W_R$  have stable inverses. Then any  $\tilde{G} \in \mathbb{RL}_\infty^{n \times m}$  satisfies  $\tilde{G} \in \mathcal{S}_A(G_0, W_L, W_R)$  if and only if

$$\begin{bmatrix} W_L W_L^* & \tilde{G} - G_0 \\ (\tilde{G} - G_0)^* & W_R^* W_R \end{bmatrix} (j\omega) \geq 0 \forall \omega \quad (5)$$

*Proof:* This is a minor variation of Theorem 1 in [5]. ■

Based on Lemma 1 the optimization in Equation 4 can be approximated on the frequency grid as:

$$\min_{G_0, W_L, W_R} \sum_{f=1}^F h(W_L, W_R, \omega_f) \quad (6)$$

subject to:

$$\begin{bmatrix} W_L W_L^* & G_k - G_0 \\ (G_k - G_0)^* & W_R^* W_R \end{bmatrix} (j\omega_f) \geq 0$$

$f = 1, \dots, F$  and  $k = 1, \dots, K$

The constraints and objective function involve product terms  $W_L W_L^*$  and  $W_R^* W_R$ . Define two new variables  $L := W_L W_L^*$  and  $R := W_R^* W_R$ . The optimization can now be expressed as a finite-dimensional SDP in terms of these new variables:

$$\min_{G_0, L, R} \sum_{f=1}^F \text{Tr}[\Gamma_L L + \Gamma_R R](j\omega_f) \quad (7)$$

subject to:

$$\begin{bmatrix} L & G_k - G_0 \\ (G_k - G_0)^* & R \end{bmatrix} (j\omega_f) \geq 0$$

$f = 1, \dots, F$  and  $k = 1, \dots, K$

The decision variables in this optimization are the complex matrices  $L(j\omega_f)$ ,  $R(j\omega_f)$ , and  $G_0(j\omega_f)$  defined at each frequency gridpoint. This can be expressed as an SDP with real matrices / constraints using a standard complex to real transformation for LMIs [12]. It is important to note that the cost function and constraints contain no coupling across the frequency gridpoints. Thus this optimization trivially decouples into  $F$  smaller SDP problems, one for each frequency gridpoint.

Equation 7 is a finite dimensional convex optimization that can be used to jointly compute the nominal model and the uncertainty weights on the frequency grid. Computational steps are described below to obtain state-space systems for the nominal model and weights. The steps are described for SISO systems  $n = m = 1$  and the extension to MIMO systems is discussed in Section III-C.

- 1) Solve Equation 7 for  $\{G_0(j\omega_f)\}_{f=1}^F$ ,  $\{L(j\omega_f)\}_{f=1}^F$ , and  $\{R(j\omega_f)\}_{f=1}^F$ . This decouples Equation 7 as  $F$  independent SDPs that can be solved with available software, e.g. LMILab in Matlab.
- 2) A state-space model for the nominal dynamics  $G_0(s)$  is fit to the optimal response  $\{G_0(j\omega_f)\}_{f=1}^F$  obtained in Step 1. This can be done in Matlab using the `fitfrd` function. The order of the state-space model is chosen by the user to obtain a trade-off between model complexity and fitting accuracy.
- 3) The state-space model  $G_0(s)$  obtained in Step 2 is substituted into Equation 7 and the optimization is resolved for  $\{L(j\omega_f)\}_{f=1}^F$ , and  $\{R(j\omega_f)\}_{f=1}^F$ . This can be done in Matlab using the `ucover` function. Step 3 reconstructs the uncertainty weights on the frequency grid to account for any error in fitting the state space nominal model.

- 4) For SISO systems,  $L := |W_L|^2$  and  $R := |W_R|^2$ . Hence the  $L(j\omega_f)$  and  $R(j\omega_f)$  obtained in Step 3 specify the magnitudes of the uncertainty weights required to cover the experimental frequency response data. Stable, minimum phase transfer functions  $W_L(s)$  and  $W_R(s)$  are constructed that satisfy  $|W_L(s)| \geq \sqrt{L(j\omega_f)}$  and  $|W_R(s)| \geq \sqrt{R(j\omega_f)}$ . This fitting step can be performed in Matlab using the `fitmagfrd` function. Constructing the state-space weights in this fashion ensures that  $\mathcal{S}_A(G_0, W_L, W_R)$  will cover the data. Moreover, the set  $\mathcal{S}_A$  is unaffected by the phase of the uncertainty weights and hence the restriction to minimum phase  $W_L$  and  $W_R$  is without loss of generality. Finally, the optimal additive uncertainty model is given by  $\mathcal{S}_A(G_0, W_L, W_R)$ .

An input multiplicative uncertainty set can be constructed starting with the optimization in Equation 4 with  $\mathcal{S}_A$  replaced by  $\mathcal{S}_M$ . The constraint in this optimization can be equivalently expressed as a frequency-dependent matrix inequality using Theorem 3 in [5]. This leads to a finite-dimensional optimization of the form:

$$\min_{G_0, W_L, W_R} \sum_{f=1}^F f(W_L, W_R, \omega_f) \quad (8)$$

subject to:

$$\begin{bmatrix} G_0 W_L W_L^* G_0^* & G_k - G_0 \\ (G_k - G_0)^* & W_R^* W_R \end{bmatrix} (j\omega_f) \geq 0$$

$f = 1, \dots, F$  and  $k = 1, \dots, K$

It is important to note that nominal model appears as products with itself and the left uncertainty weight in the upper left block of the matrix constraint. Hence this optimization is not jointly convex in  $(G_0, W_L, W_R)$  as written. As before the products of the uncertainty weights can be handled by introducing the new variables  $L := W_L W_L^*$  and  $R = W_R^* W_R$ . Further introduce  $Q_0 := G_0^{-1}$  and multiply the matrix constraint on the left and right by  $\text{diag}(G_0^{-1}, I)$  and  $\text{diag}(G_0^{-*}, I)$ . This leads to the following (convex) SDP problem:

$$\min_{Q_0, L, R} \sum_{f=1}^F \text{Tr}[\Gamma_L L + \Gamma_R R](j\omega_f) \quad (9)$$

subject to:

$$\begin{bmatrix} L & Q_0 G_k - I \\ (Q_0 G_k - I)^* & R \end{bmatrix} (j\omega_f) \geq 0$$

$f = 1, \dots, F$  and  $k = 1, \dots, K$

The numerical steps to solve for the nominal model and uncertainty weights for the input multiplicative model are essentially the same as those given above for the additive uncertainty model. The only additional detail is that the nominal model on the frequency grid  $\{G_0(j\omega_f)\}_{f=1}^F$  is obtained by inverting the values of  $Q_0(j\omega_f)$  computed from the optimization.

### C. Practical Issues

1) *Incorporating Prior Knowledge:* In many applications there is some prior knowledge regarding the nominal system dynamics. For example the voice coil motor dynamics has a double integrator characteristic, and the micro actuator has a second order high frequency roll off [13]. Let  $P(s) \in \mathbb{RL}_\infty$  denote any known characteristics of the nominal model. This prior knowledge is incorporated by constructing a nominal model of the form  $G_0(s) = P(s)T_0(s)$  where  $T_0(s)$  is the unknown component to be determined. To construct the nominal model, first transform the experimental frequency responses  $\{G_k\}_{k=1}^K$  into equivalent frequency responses for the unknown component:

$$T_k(j\omega_f) = P^{-1}(j\omega_f)G_k(j\omega_f) \forall k, f \quad (10)$$

Next, use the optimization method described previously to construct  $T_0$  and weights such that the corresponding uncertainty set covers  $\{T_k\}_{k=1}^K$ . The optimal nominal model on the frequency grid  $G_0(j\omega_f)$  is then given by multiplying the known and unknown system components, i.e.  $G_0(j\omega_f) = P(j\omega_f)T_0(j\omega_f) \forall f$ . Then the process can continue on to step 2 listed in Section B. For the optimization based on the additive uncertainty, if the optimal nominal model and uncertainty weight on the frequency grid is desired, the weight,  $W_L(j\omega_f)$  must also be multiplied by  $P(j\omega_f)$ .

2) *Limiting Magnitude of Nominal Model Derived From Multiplicative Uncertainty Set:* The uncertainty set optimization attempts to minimize the magnitude of the weights. In some cases this formulation leads to impractical results for multiplicative uncertainty sets. To illustrate the issue consider a SISO multiplicative uncertainty set  $\mathcal{S}_M(G_0, W_L, 1)$ . Systems in this set have the form  $G_0(1+W_L\Delta)$  where  $\|\Delta\| \leq 1$ . Note that this set can cover any collection of frequency responses by choosing the nominal model to have sufficiently large magnitude and  $\|W_L\| = 1$ . Thus an optimization to construct the nominal model  $G_0$  and  $W_L$  will never result in an uncertainty weight that exceeds 1 in magnitude, i.e. 100% multiplicative uncertainty is an upper bound on the optimal weight. The practical consequence is that the optimization will return a very large nominal model and an uncertainty weight of magnitude near 1 for any frequency where the responses have "large" spread. In particular, this will occur for any frequency such that  $\max_{k,l} |G_k(j\omega) - G_l(j\omega)| > 2$ . The optimization in Equation 9 can be modified to add one additional constraint that prevents the nominal model from growing too large:

$$|Q_0(j\omega_f)| \geq \min_k |G_k(j\omega_f)^{-1}| \quad (11)$$

The crux of the issue is that the actual "size" of the multiplicative uncertainty set is  $|G_0W_L|$  and the posed optimization only attempts to minimize  $|W_L|$ . It is not possible to directly minimize  $|G_0W_L|$  in a computationally efficient manner as this is a non-convex objective. An alternative procedure to construct a multiplicative uncertainty set is to first compute an additive uncertainty set and then compute the corresponding weights for a multiplicative model.

3) *Data Trimming:* In some systems, there may be prior knowledge on their uncertainty at certain frequency ranges that may not be captured by the optimization method. For example, if there is an excess of measurement noise at certain frequencies, there would be an artificially large uncertainty at those frequencies. Any prior information on the uncertainty can be incorporated by modifying the values of  $L(j\omega_f)$  and/or  $R(j\omega_f)$  at particular frequencies before fitting the state-space weights  $W_L(s)$  and  $W_R(s)$  (Step 4 in Section III-C)

4) *Fitting State-Space Models to MIMO Systems:* The optimization technique described in the previous sections can be extended to MIMO systems but some simplifications are typically required in the state-space fitting steps. For example `fitfrd` in Matlab applies only for vector systems (either one input or one output). Thus in the case of a MIMO system, one possible method is to fit a state-space model to the data one column or one row at a time. This method will naturally increase the order of the MIMO system, thus utilizing some order reduction technique may be useful. For the uncertainty weights, the fitting process is simplified by restricting the weights, a priori, to be diagonal.

### D. Simple Numerical Example

In this example, a stable second order system with uncertainties in its natural frequency and damping ratio is used to demonstrate the approach described in the previous section. First a transfer function with uncertainty is defined as,

$$G_{true}(s) = \frac{p^2}{s^2 + 2\zeta p + p^2} \quad (12)$$

where  $\zeta = [0.05, 0.1]$  and  $p = [3, 7]$ . In a real application the true underlying model, specified here by  $G_{true}$  would not be known. The "true" model is defined here to generate the frequency response data that is used in the proposed model uncertainty construction procedure. An uncertainty set such as  $\mathcal{S}_A(G_0, W_L, 1)$  does not capture the parametric uncertainties that appears in the true model but it is still useful for creating a robust controller for a system like this.

Experimental data  $\{G_k\}_{k=1}^K$  was simulated by taking  $K = 100$  random samples of  $\zeta$  and  $p$  with a frequency containing 250 frequency points from  $\omega_1 = 10^{-1}$  rad/sec to  $\omega_{250} = 10^2$  rad/sec. Since the magnitude difference between the different  $G_k(j\omega_f)$  was too large, the nominal model was constructed using the LMI constraints for an additive uncertainty and then the multiplicative uncertainty weight for the  $G_0(j\omega_f)$  was constructed using the method described in section III-C.2. A second nominal model was created by taking the average of  $G_k(j\omega_f)$  and utilizing `ucover` to create the  $W_L(j\omega_f)$  for this model. It is known that the average of plant models is not the best nominal model for robust controller design, thus this example was created to show the advantage of the nominal model created from the LMI constraints. Fig. 2 shows the resultant frequency response data of the two nominal models, and the smallest multiplicative uncertainty weight required to cover all of the experimental data.

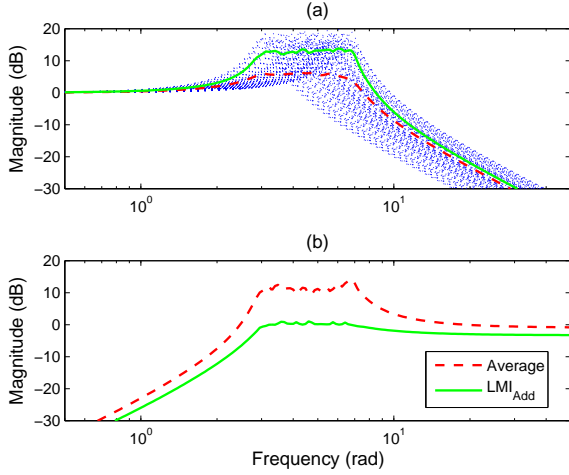


Fig. 2. (a) The nominal model,  $G_0(j\omega)$  created from the additive uncertainty optimization method and averaging of the simulated data (b) The smallest multiplicative uncertainty weight,  $W_L$  to cover all of the experimental data.

As shown in the bottom subplot of Fig. 2, the uncertainty weight for the average system is greater than the uncertainty weight for the nominal model created by the optimization method. Since there are uncertainties in both  $\zeta$  and  $p$  values, the frequency and magnitude of the peak are different for each sample. Since only 1 peak exists for each frequency response data, when the average of the samples are taken the magnitude of the peak of each sample is reduced by  $K - 1$  other frequency response data.

For a SISO system the LMI constraint finds a complex number at each frequency that will require a circle with the smallest radius to cover all of the data points. This point is exemplified in Fig. 3, which shows a scatter plot of the simulated data, two nominal data points, and the smallest circle centered at each of the nominal data points required to cover all of the data points at  $\omega = 5$  rad/sec. At this frequency many of the data points are near the real axis, and thus the average of the data is naturally pushed up towards the real axis. The nominal point created by the averaging method requires a circle with a radius of 6.5 to cover all of the data, while the nominal point created using the optimization method requires a circle with a radius of 4.3 to cover all of the data. Compared to the average model the nominal model derived from the LMI constraint requires an uncertainty weight with smaller magnitude to cover the frequency response data, which should result in a controller with better performance.

#### IV. RESULTS

The proposed algorithm was tested using 27 frequency responses obtained on different dual-stage HDD. As shown in Fig. 1, the voice coil motor and the micro actuator work together to keep the magnetic head at a desired position. The block diagram for the uncertainty system of a dual-stage actuator with input multiplicative uncertainty is shown in Fig. 4. The inputs,  $u_{VCM}$  and  $u_{MA}$ , to the actuators are

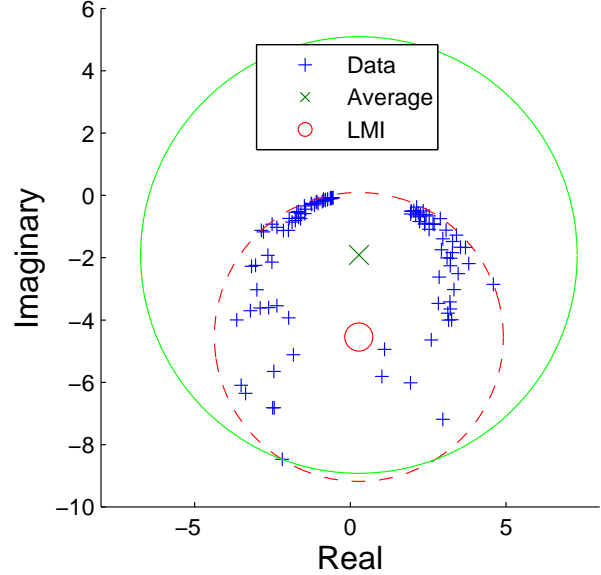


Fig. 3. The data points and the nominal point created by LMI method and Averaging method at  $\omega=5$ rad/sec.

typically voltage or current signals from the HDD controllers. The  $W_1$  and  $W_2$  are uncertainty weights for the VCM and MA system, respectively. The magnetic head determines its position by computing the position error signal (PES) from signals on the magnetic disk. The frequency response data is extracted from a drive by injecting sinusoidal signals as disturbance signals and recording the PES at each frequency. Although this method requires less than 1 minute to obtain the frequency response data of both the VCM and MA systems, at low frequency there is a large variation between the different HDD data due to measurement noise.

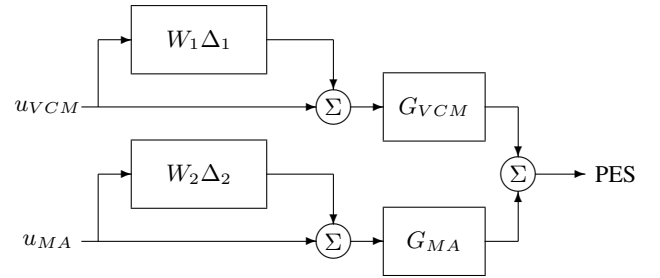


Fig. 4. The block diagram for the uncertainty system of a dual-stage actuator.

From the 27 frequency response data, the uncertainty model for the dual-stage actuator as depicted in Fig. 4 was constructed utilizing optimization technique described in this paper. Many of the techniques from section III-C were utilized to create the uncertainty model. First, the VCM is essentially a double integrator at low frequencies (below the first flexible mode) due to the rigid-body rotational dynamics. Moreover, the MA is known to have a high frequency second-

order roll-off and a gain of 0 dB at low frequencies. The method from Section III-C was used to incorporate these known dynamics in the nominal models. Second, it is known that the low-frequency data has high variance due to the measurement noise introduced during the sinusoidal sweep. The optimal uncertainty weights were reduced at these frequencies. Furthermore data points were added beyond  $\omega_F$  with magnitude of  $W_L(j\omega_F)$  to prevent the state-space model fit from rolling down at high frequency. The LMI constraint based on  $\mathcal{S}_A(G_0, W_L, 1)$  was used to construct the optimal nominal model, while LMI constraint based on  $\mathcal{S}_M(G_0, W_L, 1)$  was utilized to construct the optimal input multiplicative uncertainty weight. An 8<sup>th</sup> order fit was used to create  $G_0(s)$  for both the actuators, and a 5<sup>th</sup> order fit was used for  $W_1(s)$  and  $W_2(s)$ .

Fig. 5 and Fig. 6 show the experimentally recorded frequency response data of VCM and MA and the uncertainty model derived from the data respectively. For confidentiality purposes, the magnitude and frequency axes have been normalized. Both the magnitude and the phase of the VCM and MA nominal models are shown in black solid lines, while the upper and lower bounds created from their respective uncertainty weights are shown in red dotted lines. The cloud of light blue lines is the collection of experimental data. The lower bound magnitude falls to zero and the bounds on the phase uncertainty cover  $[-180^\circ, 180^\circ]$  once the multiplicative uncertainty weight exceeds 1, which occurs at  $\omega > 40$  and  $\omega > 46$  for the VCM and DAC respectively. Thus the corresponding bound curves are not shown for frequencies where the weight magnitude exceeds 1. It is worth noting that the closed-loop bandwidth of the system is bounded by these frequencies since the phase of the uncertainty model covers the entire unit circle once  $|W_L| > 1$ . In Fig.5, the double integrator characteristics can be seen as it was incorporated into the system model. The maximum and minimum magnitude and phase at low frequency for both VCM and MA do not bound all of the experimental data, since the uncertainty weight at low frequency was reduced due to occurrence of measurement noise. Furthermore the maximum magnitude of both VCM and MA system do not "tightly" cover the experimental data, since low order fit was used to create the uncertainty weights. Higher order systems could be used to improve the fits but this would ultimately increase the order of the system and hence the complexity of the control design. This is also true for increasing the order of the nominal models. Since there is limited computational power on the HDD controller, it is desired to design a low order controller and thus minimal orders are used to create the uncertainty model.

The uncertainty models can be used within the interconnected model as shown in Fig. 7 in order to construct a robust controller via  $\mu$ -synthesis [3].  $P_{unc}$  is the uncertainty model shown in Fig. 4,  $W_D$  is the disturbance weight,  $W_P$  is the performance weight, and  $W_V$  and  $W_M$  are the actuator weights for the VCM and MA. For  $W_P$  and  $W_D$  a low pass filter was utilized, while the actuator weights utilized a constant value and a low pass filter for  $W_V$  and  $W_M$ ,

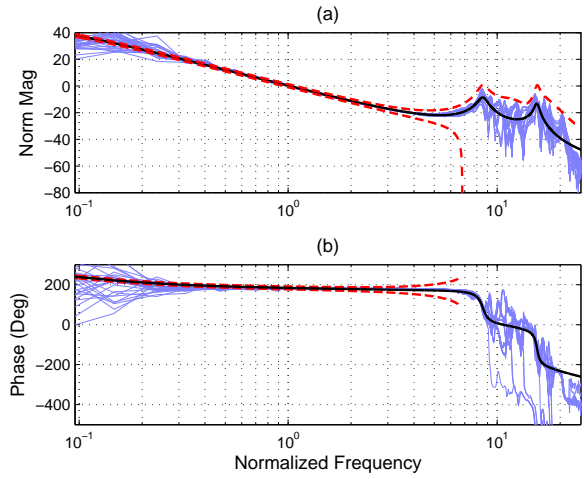


Fig. 5. (a) The magnitude of the nominal VCM model (solid line) created from the LMI constraint shown with the upper and lower bound (dotted line). (b) The phase of the nominal VCM model (solid line) created from the LMI constraint shown with the upper and lower bound (dotted line).

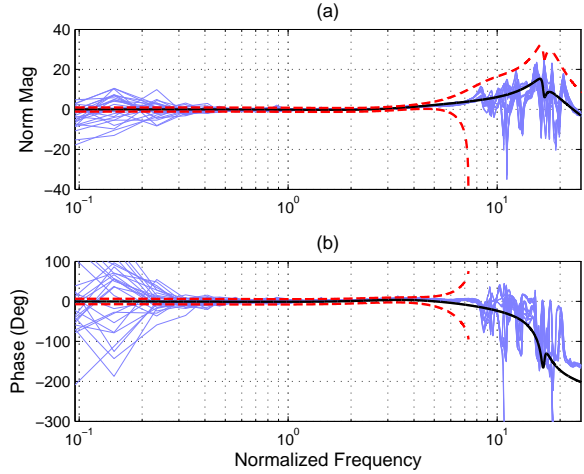


Fig. 6. (a) The magnitude of the nominal MA model (solid line) created from the LMI constraint shown with the upper and lower bound (dotted line). (b) The phase of the nominal MA model (solid line) created from the LMI constraint shown with the upper and lower bound (dotted line).

respectively to prioritize the usage of MA for high frequency inputs.

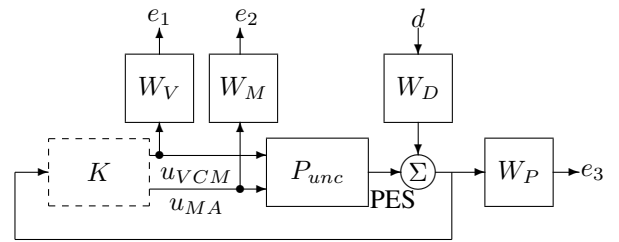


Fig. 7. The interconnected model used to create a robust controller,  $K(s)$

A controller was synthesized with `dksyn` and the result is an 76th-order controller. This controller was reduced

to 20-states using balanced truncation. The reduced-order controller was assessed by computing the closed-loop sensitivity function as well as classical gain/phase margins using the experimental open-loop frequency response data. The controller was then implemented on a dual-stage HDD from the same product-line as those used to generate the 27 frequency responses. The open loop response and closed-loop sensitivity function were measured by injecting sinusoids at various frequencies. The experimental results, shown in Fig. 8, demonstrate that the automatically generated uncertainty set can be used to construct robust control designs for a dual-stage actuator of a HDD.

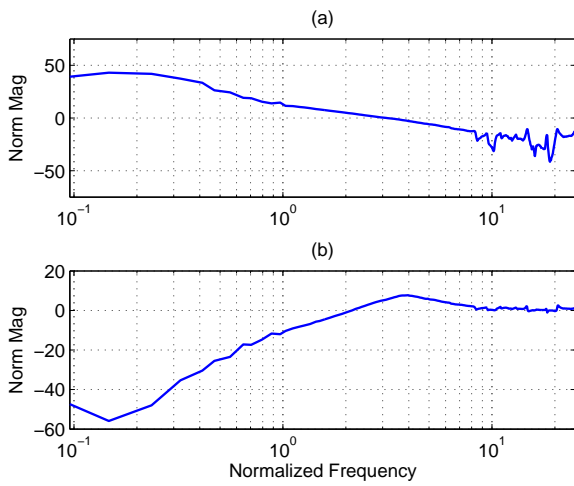


Fig. 8. (a) Experimental Open Loop Response (b) Experimental Sensitivity Function

## V. CONCLUSION

A practical method of creating an uncertainty set for a dual-stage actuator of hard disk drives from a set of experimental frequency response data was presented in this paper. The numerical algorithm was derived through definitions of additive and input multiplicative uncertainty sets. Furthermore this method was altered for the practical application of robust controller synthesis for a dual-stage actuator of a hard disk drive. A robust controller was synthesized using

the uncertainty model derived from the proposed method and tested on a hard disk drive successfully. Future work will include applying the method onto the dual-stage actuator as a 2 input 1 output system, instead of dealing with the system as two separate SISO systems.

## VI. ACKNOWLEDGMENT

This work was supported by Seagate under a grant entitled "Robust Control Design for Hard Disk Drives." The authors also acknowledge useful discussions with engineers at Seagate including Raye Sosseh and Chiyun Xia.

## REFERENCES

- [1] R. Wood, "Future hard disk drive systems," *Journal of magnetism and magnetic materials*, vol. 321, no. 6, pp. 555–561, 2009.
- [2] "Exceeding capacity, speed and performance expectations: Seagate AcuTrac technology defines new standards," tech. rep., Seagate, 2011.
- [3] S. Skogestad and I. Postlethwaite, *Multivariable Feedback Control: Analysis and Design*. John Wiley & Sons, 2005.
- [4] H. Hindi, C.-Y. Seong, and S. Boyd, "Computing optimal uncertainty models from frequency domain data," in *Decision and Control, 2002, Proceedings of the 41st IEEE Conference on*, vol. 3, pp. 2898–2905, 2002.
- [5] G. Balas, A. Packard, and P. Seiler, "Uncertain model set calculation from frequency domain data," in *Model-Based Control* (P. M. Hof, C. Scherer, and P. S. Heuberger, eds.), pp. 89–105, Springer US, 2009.
- [6] K. Häggblom, "Data-based uncertainty modeling by convex optimization techniques," in *Proc. Int. Symp. Advanced Control of Chemical Processes*, pp. 91–96, 2006.
- [7] K. Häggblom, "Data-based modeling of block-diagonal uncertainty by convex optimization," in *IEEE American Control Conference*, pp. 4637–4642, 2007.
- [8] K. Häggblom, "Convex formulations for data-based uncertainty minimization of linear uncertainty models," in *Control Automation Robotics & Vision (ICARCV), 2010 11th International Conference on*, pp. 501–505, IEEE, 2010.
- [9] K. Häggblom, "MIMO uncertainty model identification of time-delay systems," in *Advanced Control of Chemical Processes*, vol. 8, pp. 385–390, 2012.
- [10] S. Boyd, L. El Ghaoui, E. Feron, and V. Balakrishnan, *Linear Matrix Inequalities in System and Control Theory*, vol. 15 of *Studies in Applied Mathematics*. SIAM, 1994.
- [11] K. Zhou, J. Doyle, and K. Glover, *Robust and Optimal Control*. Prentice-Hall, 1996.
- [12] S. Boyd, L. El Ghaoui, E. Feron, and V. Balakrishnan, *Linear Matrix Inequalities in System and Control Theory*, vol. 15 of *Studies in Applied Mathematics*. SIAM, 1994.
- [13] J. Zheng, M. Fu, Y. Wang, and D. C., "Nonlinear tracking control for a hard disk drive dual-stage actuator system," *Transactions on Mechatronics*, 2008.